IEEE Access
Multidisciplinary | Rapid Review | Open Access Journal

Received November 6, 2019, accepted December 27, 2019, date of publication January 6, 2020, date of current version January 28, 2020.

*Digital Object Identifier 10.1109/ACCESS.2020.2964335*

# Lorenz Curve-Based Entropy Thresholding on Circular Histogram

**CHAO KANG, CHENGMAO WU, AND JIULUN FAN**
School of Communication and Information Engineering, Xi'an University of Posts and Telecommunications, Xi'an 710121, China
School of Electronic Engineering, Xi'an University of Posts and Telecommunications, Xi'an 710121, China

Corresponding author: Chao Kang (1015584136@qq.com)

This work was supported by the National Natural Science Foundation of China under Grant 61671377.

**ABSTRACT** Circular histogram thresholding is a new threshold selection method in color image segmentation. However, the method of the existing circular histogram thresholding based on the Otsu Criteria lacks the generality of using the circular histogram. In order to improve the effectiveness and reduce the complexity of thresholding on circular histogram, this paper firstly introduces the Lorenz curve into circular histogram. Then the circular histogram is expanded into the linearized histogram in clockwise or anti-clockwise direction by the optimal index of the Lorenz curve. In the end, the entropy thresholding of the linearized circular histogram is adopted to choose the optimal threshold to obtain the object of color images. Many experimental results show that the proposed method has better effectiveness and adaptability than the existing circular thresholding utilizing Otsu Criteria.

**INDEX TERMS** Color image segmentation, circular histogram thresholding, entropy method, Lorenz-curve type technique.

## I. INTRODUCTION

Target acquisition of color image is an important problem in image analysis, understanding and computer vision due to the color images can provide more information than gray-level images. Color image segmentation [1], [2] has made profound effects to color information analysis, for which the RGB color space is the most used [1]–[3] with three primary colors: red (R), green (G) and blue (B). Also, other color representations can be derived from RGB color space, such as HSI, CIE, YIQ color spaces and so on.

However, among all color spaces, RGB is not suitable for the color image segmentation due to the high correlation among the three components [3]. Conversely, HSI color space [2], [4] has been used more frequently due to three highly irrelevant components: hue (H), saturation (S) and intensity (I). Many researchers had used the HSI color space in the color images' segmentation [4]–[7] due to this model which can represent hue information and has a more natural correspondence to human vision than the RGB color model. Among them, segmenting the images only by H component is an important approach. The angle value of hues increasing from 0° to 359° can be used adequately (Note that we leave out the angle symbol (°) for the convenience in the following). This color model can establish a circular function with periodicity and continuity.

Thresholding H component is first studied by Tseng *et al.* [8], Wu *et al.* [9], Dimov and Laskov [10] and Lai and Paul [11]. Among them, Lai and Paul [11] had proposed an efficient circular histogram thresholding based on Otsu's method [12] taking $O(L)$ time, and applied this model on optical flow data, indoor/outdoor image classification and non-photorealistic rendering, where $L$ is the number of the histogram bins. One interest property of Otsu's method expressed by within-class variance on circular histogram thresholding using linear statistic is proved.

This circular thresholding model had assumed that the distribution of circular histogram satisfying satisfies the Gaussian distribution. However, not all the distributions of hues can ideally satisfy the Gaussian distribution. Furthermore, the color defined in the HSI color model is one of examples of data in cylindrical coordinates, and using Euclidean distance may result in an inappropriate analysis of the samples [13]. Because the hue value forms a periodic distribution, the Euclidean distance used in the existed circular thresholding [11] may not obtain the meaningful data [13]. Also, the

The associate editor coordinating the review of this manuscript and approving it for publication was Chaker Larabi.

Otsu Criteria assumes the distributions of the two classes of the histogram are Gaussian distribution, and the sizes of them are nearly similar [14]–[16]. There exists a limitation of the Otsu Criteria whether on the circular histogram or the linear one.

In that case, the Otsu method used in literature [11] may have the problem. In order to adapt gray-level thresholding methods appropriately on this periodic distribution, we use entropy thresholding on this circular thresholding model [11]. The entropy method [17] has been used more frequently in image segmentation, due to it is dependent only on the uniformity of the samples rather than distribution of the histogram. However, we found the entropy-based circular histogram thresholding takes $O(L^2)$ time for binary thresholding.

However, In fact, the brute force search is used directly on the existing model [11] in the entropy-based circular histogram thresholding taking $O(L^2)$ time (taking $O(L^2)$ time) in single-threshold cases, and the complexity of entropy thresholding on circular histogram would be $O(L^2), O(L^3), \ldots, O(L^{n+1})$ for $n$ level-threshold cases. The complexity of this entropy-based circular thresholding is too high, which cannot meet the real-time requirement in Industrial Automation fields, Intelligence traffic systems, and Machine Vision fields and so on. Therefore, in order to reduce the complexity of entropy-based circular thresholding and make it more adaptable to be extended to multi-thresholding cases, we aim to break the circular histogram into the linearized one and obtain the optimal threshold on that. In that case, the complexity of entropy thresholding on the linearized histogram expanded from the circular histogram now takes $O(2L)$ time in single-threshold case, and that would be reduced to $O(2L), O(L^2), \cdots, O(L^n)$ for $n$ level-threshold cases, where $L$ is the number of the histogram bins.

The circular histogram of H component is not usually like the gray-scale linear one histogram with the fixed starting point (0) and the terminal point (255). The difference between two histograms is that the change of hue levels is not equivalent to that of the gray levels using linear statistic. Furthermore, the starting point of the circular histogram can be at any position on that.

In order to effectively select the optimal breakpoint to break the circular histogram, the Lorenz curve technique [18] is introduced. Lorenz curve method has been proposed by American statistician Lorenz in 1907 in economics to study the distribution of national income among nationals. Researchers have used Lorenz curve more frequently in analyzing the distribution uniformity of samples value [19]–[23]. Hence, considering the nice property of the Lorenz curve, we will apply this method on entropy-based circular thresholding.

The organizational structure of this paper is as follows. The basis of the existed circular thresholding model is given in Section 2. Section 3 describes the entropy method on the existed circular thresholding model. Section 4 introduces the theory for breaking the circular histogram based on the Lorenz curve technique. The entropy method on the linearized histogram is described in Section 5. Section 6 shows the experimental results and the analysis. See section 7 for conclusions.

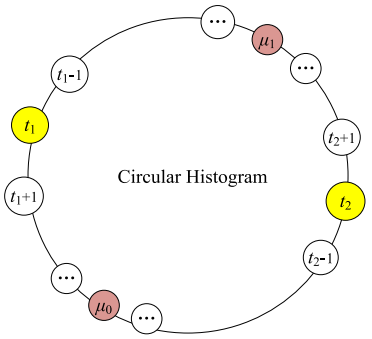


**FIGURE 1.** Circular histogram thresholding based on Otsu method.

## II. RESEARCH BASIS

Lai and Paul [11] had introduced an efficient method of using binary thresholding on circular histogram taking $O(L)$ time, where $L$ is the number of the histogram bins. The principle of the Otsu-based circular histogram thresholding is shown as Fig. 1.

Thresholding on circular histogram proposed in literature [11] is different from that on linear histogram case, the former needs two thresholds $(t_1, t_2)$ to partition the histogram into two portions as shown in Fig. 1. The first threshold is used to select the appropriate starting point, and the second one is to segment the two portions $(t_1..t_{2-1})$ and $(t_2..t_{1-1})$.

The circular sum is defined as $\overset{\circ}{\sum}_{t=t_1}^{t_2}$ :

$$\overset{\circ}{\sum}_{t=t_1}^{t_2} = \begin{cases} \sum_{t=t_1}^{t_2} & \text{if } t_1 \le t_2 \\ \sum_{t=t_1}^{L-1} + \sum_{t=1}^{t_2} & \text{if } t_1 > t_2 \end{cases} \tag{1}$$

The circular histogram $\{h(t)\}$ satisfies $\sum_{t=0}^{L-1} h(t) = 1(h(t) \ge 0), t = 0, 1, \ldots, L-1$, we have the following formula based on Otsu criteria:

The probability $P_0$, means $\mu_0$ and within-class variance $\sigma_0^2$ of portion 1 is defined as:

$$P_0(t_1, t_2) = \overset{\circ}{\sum}_{t=t_1}^{t_2-1} h(t), \tag{2}$$

$$\mu_0(t_1, t_2) = \frac{\overset{\circ}{\sum}_{t=t_1}^{t_2-1} th(t)}{P_0(t_1, t_2)}, \tag{3}$$

$$\sigma_0^2(t_1, t_2) = \frac{\overset{\circ}{\sum}_{t=t_1}^{t_2-1} h(t)(t \overset{\circ}{-} \mu_0(t_1, t_2))^2}{P_0(t_1, t_2)}. \tag{4}$$

The probability $P_1$, means $\mu_1$ and within-class variance $\sigma_1^2$ of portion 2 is defined as:

$$P_1(t_1, t_2) = \overset{\circ}{\sum}_{t=t_2}^{t_1-1} h(t), \tag{5}$$

$$\mu_1(t_1, t_2) = \frac{\overset{\circ}{\sum}_{t=t_2}^{t_2-1} th(t)}{P_1(t_1, t_2)}, \tag{6}$$

$$\sigma_1^2(t_1, t_2) = \frac{\overset{\circ}{\sum}_{t=t_2}^{t_1-1} h(t)(t \overset{\circ}{-} \mu_0(t_1, t_2))^2}{P_1(t_1, t_2)}. \tag{7}$$

Probabilities $P_0$ and $P_1$ satisfies the relations:

$$P_0(t_1, t_2) + P_1(t_1, t_2) = \overset{\circ}{\sum}_{t=t_1}^{t_1-1} h(t) = \sum_{t=0}^{L-1} h(t) = 1$$

and $P_0(t_1, t_2)\mu_0(t_1, t_2) + P_1(t_1, t_2)\mu_1(t_1, t_2) = \mu_T$, where $\mu_T = \overset{\circ}{\sum}_{t=t_1}^{t_2-1} th(t) + \overset{\circ}{\sum}_{t=t_2}^{t_1-1} th(t) = \sum_{t=0}^{L-1} th(t)$ is the total means.

Lai and Paul [11] had demonstrated that the within-class variance $\sigma_W^2$ showed a better segmentation effect than that of $\sigma_B^2(\sigma_T^2 \neq \sigma_W^2 + \sigma_B^2$ on circular histogram). Lai *et al.* had proved that the optimal search using $\sigma_W^2$ can be only on $t_1$ and $t_2$ is obtained by $|t_2 \overset{\circ}{-} t_1| = L/2$ (when $L$ is even). This optimal search of linear statistic takes $O(L)$ time unlike the brute force search of circular statistic taking $O(L^2)$ time.

So the within-class variance $\sigma_W^2(t_1, t_2)$ is obtained:

$$\begin{aligned}\sigma_W^2(t_1, t_2) &= P_0(t_1, t_2)\sigma_0^2(t_1, t_2) + P_1(t_1, t_2)\sigma_1^2(t_1, t_2) \qquad (8)\\ &= \overset{\circ}{\sum}_{t=t_1}^{t_2} h(t)(t \overset{\circ}{-} \mu_0(t_1, t_2))^2 \\ &\quad + \overset{\circ}{\sum}_{t=t_2+1}^{t_1-1} h(t)(t \overset{\circ}{-} \mu_1(t_1, t_2))^2. \qquad (9)\end{aligned}$$

The between-class variance $\sigma_B^2$ is obtained as:

$$\sigma_B^2(t_1, t_2) = P_0(t_1, t_2)\mu_0^2(t_1, t_2) + P_1(t_1, t_2)\mu_1^2(t_1, t_2), \tag{10}$$

We can see that $\sigma_T^2 \neq \sigma_W^2 + \sigma_B^2$ on circular histogram, where $\sigma_T^2(t, t) = \overset{\circ}{\sum}_{t=t_1}^{t_1-1} (t - \mu_T)^2$ is the total variance.

For the convenience, the circular difference $\overset{\circ}{-}$ denotes $a \overset{\circ}{-} b = (a - t_1) \bmod L - (b - t_1) \bmod L$, $p \bmod q$ gives a non-negative integer that has the remainder as $p$ divided by $q$. The main idea of this circular calculation can be taken as measuring the difference between two points after rotating the histogram and then $t_1$ becomes the first point on the histogram.

The optimal thresholds $(t_1^*, t_2^*)$ are obtained by minimizing the within-class variance $\sigma_W^2(t_1, t_2)$ [11]:

$$(t_1^*, t_2^*) = Arg \min_{0 \le t_1, t_2 \le L-1} \sigma_W^2(t_1, t_2), \tag{11}$$

The processes of circular thresholding are [11]:

1) Denoting all possible starting points $t_1 = 0, 1, \ldots, L-1$ on circular histogram.
2) Once a starting point $t_1$ is selected, the optimal threshold $t_2$ is obtained by $t_2 = (t_1 + L/2) \bmod L$, where $L$ is even in this paper.
3) Select the optimal threshold values $(t_1^*, t_2^*)$ such that the with-class variance $\sigma_W^2(t_1, t_2)$ on circular histogram is minimal.

This efficient circular thresholding model optimized the binary thresholding $(t_1, t_2)$ on circular histogram. The model had equally divided histogram by the constrain $|t_2 \overset{\circ}{-} t_1| = L/2(L$ is even) to reduce the complexity of binary thresholding from $O(L^2)$ to $O(L)$.

However, the thresholds $(t_1^*, t_2^*)$ selected by (11) may not be the most optimal due to the complexity and periodicity of the circular histogram. That is, because the constrain $|t_2 \overset{\circ}{-} t_1| = L/2(L$ is even) may not be able to be extended to general cases. That is, an equal division of the hue level on circular histogram may not always be ideal [14]–[16].

The measurement using Euclidean distance is reasonable for a data, which is sampled from an isotropic Gaussian distribution. However, we cannot always obtain a good result on circular histogram because the distribution of elements of the hue data does not meet the isotropic Gaussian distribution [15]. In that case, considering the special distribution of hue component in HSI color space, we adapt the entropy thresholding to the existed circular thresholding [11]. The entropy thresholding requires no Euclidean distance measurement, and the distribution of the samples for thresholding is not considered.

## III. ENTROPY THRESHOLDING METHOD

In this section, we will briefly introduce the entropy thresholding on linear histogram, and then we use this method on circular histogram based on the existing circular thresholding model [11].

### A. TRADITIONAL ENTROPY THRESHOLDING METHOD

Entropy [17] based on information theory is a measurement of the uncertainty of a random variable, and the entropy is the larger, random variables are the more uncertain. The maximum entropy thresholding method has been used more frequently in image segmentation, and the uniformity of the distribution is the only index.

This maximum entropy model is that when we need to predict the probability distribution of a random event, our prediction should meet all known conditions, and do not make any subjective assumptions for the unknown situation. It's important not to make subjective assumptions. In this case, the probability distribution is the most uniform and the predicted risk is the least. The information entropy of probability distribution now is the largest.

This measurement seems to be more global and also of more general to need no any of the prior knowledge about the picture other than the grey-level histogram itself.

Let $G$ denotes the gray levels $G = [0, 1, \ldots, L-1]$ of a 2D image, and the histogram of the image be $h(g)$. Thereby, the entropy $H(g)$ of the histogram is achieved as:

$$H(g) = -\sum_{g=0}^{L-1} h(g) \log h(g). \tag{12}$$

In the two-class case, the threshold is denoted as $t$ to divide the histogram into two portions $C_0(t)$ and $C_1(t)$.

The first portion is $C_0(t) = \{0, 1, \ldots, t\}$ and the second one is $C_1(t) = \{t+1, t+2, \ldots, L-1\}$. The cumulative probability of the two parts:

$$P_0(t) = \sum_{g=0}^{t} h(g), \tag{13}$$

$$P_1(t) = \sum_{g=t+1}^{L-1} h(g). \tag{14}$$

The entropy of the entire image objective function $H_T(t) = H_0(t) + H_1(t)$ is obtained:

$$\begin{aligned} H_T(t) &= H_0(t) + H_1(t) \\ &= -\sum_{g=0}^{t} \frac{h(g)}{P_0(t)} \log \frac{h(g)}{P_0(t)} - \sum_{g=t+1}^{L-1} \frac{h(g)}{P_1(t)} \log \frac{h(g)}{P_1(t)}. \end{aligned} \tag{15}$$

Therefore, the optimal threshold $t^*$ of entropy thresholding is:

$$t^* = \arg \max_{0<t<L-1} H_T(t). \tag{16}$$

Considering the good nature of the entropy Criteria, we used the entropy method on the existed circular thresholding model [11].

### B. ENTROPY-BASED CIRCULAR HISTOGRAM THRESHOLDING

In order to process the circular histogram with the periodic distribution appropriately, we adapt the entropy thresholding on circular histogram. However, the optimal search model of $|t_2 -^{\circ} t_1| = L/2$ ($L$ is even) is not suitable for entropy thresholding because it is obtained from Otsu Criteria [14]–[16]. Thereby, the brute force search now is used for binary thresholding.

Therefore, based on the model of the Otsu-based circular thresholding [11], the threshold $t$ also divides the histogram into two partitions $(t_1, t_2 - 1)$ and $(t_2, t_1 - 1)$. The first threshold $t_1$ is used to select the appropriate starting point, and the second one $t_2$ now is used to identify the position where the entire entropy can achieve the maximum value.

The entropy $H_0(t_1, t_2)$ of the portion 1 is obtained as:

$$H_0(t_1, t_2) = -\sum_{t=t_1}^{t_2-1 \circ} \frac{h(t)}{P_0(t_1, t_2)} \log \frac{h(t)}{P_0(t_1, t_2)}, \tag{17}$$

The entropy $H_1(t_1, t_2)$ of the portion 2 is obtained as:

$$H_1(t_1, t_2) = -\sum_{t=t_2}^{t_1-1 \circ} \frac{h(t)}{P_1(t_1, t_2)} \log \frac{h(t)}{P_1(t_1, t_2)}, \tag{18}$$

where the $P_0(t_1, t_2)$ and $P_1(t_1, t_2)$ are the cumulative probability of the two portions same as formula (2) and (5).

The entropy of the entire image is

$$H_T(t_1, t_2) = H_0(t_1, t_2) + H_1(t_1, t_2).$$

So the optimal thresholds are obtained:

$$(t_1^*, t_2^*) = \arg \max_{0 \le t_1, t_2 \le L-1} H_T(t_1, t_2). \tag{19}$$

However, this model takes $O(L^2)$ time, so that this circular thresholding model may lack the adaptability, where $L$ is the number of the histogram bins.

Hence, it is necessary to modify this circular thresholding model and in order to reduce the complexity of entropy-based circular thresholding, so we use a specific method to achieve the linearized histogram based on the constrain that the new linearized histogram maintains the original distribution.

## IV. CIRCULAR HISTOGRAM'S LINEARIZING METHOD

In this section, we will firstly introduce the Lorenz curve and give a theoretical explanation that the circular histogram can be expanded into a linear histogram. Then, we propose our method using Lorenz curve technique to select the optimal breakpoint on circular histogram as the starting point of the linearized histogram.

### A. LORENZ CURVE

Lorenz curve has provided a new analysis method for wide application and popularization, especially for image processing in recent years. Kittler and Illingwotth [16] had measured the texture segmentation problems with Gini index. Kapur *et al.* [17] had measured the pixels homogeneity within each segmented region by Gini index. Joseph *et al.* [18] have calculated the diagnosis of a lung nodule in computerized tomography images. The sparsity measurement of a network graph based on the Gini index is proposed by Shih and Liu [19]. Cote and Albu [20] had determined whether the received image is changed by noise or artificial tampering using Lorenz curve. Habba *et al.* [21] had proposed an image contrast enhancement method by the uniformity reflected by the Lorenz curve.

The uniformity of cumulative probability distribution reflected by Lorenz curve is a highly effective way to measure the changing trend of any algorithm.

Denoting $\{h(x)\}$ ($\sum_{-\infty}^{+\infty} h(x)dx = 1$, $h(x) \ge 0$) as the probability density representing the distribution of a sample set $\{x\}$, (note that we only consider the $x \ge 0$ situation).

Denoting $P(x)$ as cumulative probability distribution of the samples, where $0 \le P(x) \le 1$, $\forall a < b, P(a) \le P(b)$, so:

$$P(x) = \int_0^x h(t)dt, \tag{20}$$

Lorenz curve is denoted as $L(P(x))$ is described as Fig. 2, which is defined as the ratio of the sum of all sample values that are less than $x$ to all samples in a set, that is:

$$L(P(x)) = \frac{\int_0^x th(t)dt}{\int_0^1 th(t)dt.} \tag{21}$$

As Fig. 2 demonstrates that the radian of the curve is related to the distribution of all sample values in the set. The greater the difference between the distributions of sample values,

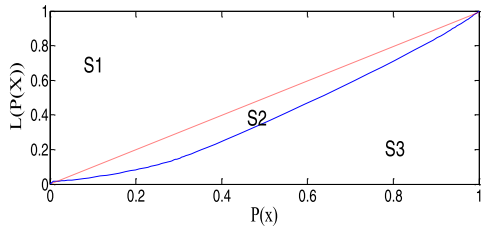


**FIGURE 2.** Lorenz curve.

the greater the radian of the Lorenz curve. A line in red from (0, 0) to (1, 1) in Fig. 2 shows the curve of zero radian with the same values of all samples in a set. We can see that the entire area of Fig. 2 is divided into three pieces $S_2 + S_3 = S_1$.

### B. CRITERIA FOR BREAKING CIRCULAR HSITOGRAM

#### 1) Breaking PRINCIPLE

In order to effectively select the breakpoint, we aim to select one of the linearized histograms which can still maintain the original distribution. In that case, the circular histogram's expansion is reasonable when the original distribution still remains as described in Fig. 3. (Note that in Fig. 3, the hue level has been quantized to 256 levels).

Considered the specific property of the dynamic starting and the terminal point within the interval on circular histogram, the basic thought of the circular histogram's expansion is that we first one breakpoint is that the first breakpoint $t_1$ is selected on circular histogram, and then the broken histogram is expanded into the linearized histogram with the selected breakpoint $t_1$ as the starting point (0).

Fig. 3 shows a circular histogram's expansion process at four random points, we can see that the four breakpoints 30, 50, 70, 100 are used as the starting point of the linearized histogram. However, from Fig. 3(b), (c) and (d), we can observe that different breakpoints on circular histogram can break the original distribution into different distributions. Among these four linearized histograms, Fig. 3(e) shows the distribution similar to that of Fig. 3(a) with a small peak at low level. Fig. 3(f) is the most ideal histogram that we aim to obtain from the original histogram with the breakpoint $t_1$ as the starting point.

Therefore, there can be one appropriate breakpoint within 256 positions to obtain the histogram most similar to the original distribution as Fig. 3(a). Thereby, we can break the circular histogram into the linearized one.

#### 2) SELECTION BY AREA DIFFERENCE

Considering the good property of the Lorenz curve, we use this curve to select the optimal histogram from all the 256 kinds256 kinds of histograms, most similar to the original distribution on circular histogram from which most similar to the original distribution on circular histogram. In this section, we firstly use the Lorenz statistic on different 256 linearized histograms, and then chose the histogram based on the optimal area difference.

We extend this curve to H component of HSI color space. Based on the linearized histogram with the breakpoint $t_1$ in ACW anti-clockwise (ACW) direction case as an example, the Lorenz curve $L(P)$ now is obtained as:

$$L(P(r, t_1)) = \frac{\int_{t=0}^{r} th(t, t_1)dt}{\int_0^1 th(t, t_1)dt}, \tag{22}$$

and the cumulative probability $P(r, t_1)$ of the H component is:

$$P(r, t_1) = \sum_{t=0}^{r} h(t, t_1) \tag{23}$$

where $r = (t + t_1) \bmod 256$, $t, t_1 \in \{0, 1, \ldots, L-1\}$.

From Fig. 2 we can know the smaller the area $S_3$ is, the larger the area $S_2$. If the curve is close to the dotted line, the distribution of the cumulative probability of H component is much evener.

The corresponding Lorenz curves to the linearized histograms from Fig. 3 (b)-(e) are described in anti-clockwise (ACW) ACW direction as shown in Fig. 4.

In order to identify the appropriate linearized histogram in Fig. 2, we use the area difference parameter $\delta(P)$ to reflect the change of the area, which is defined as:

$$\begin{aligned} \delta(P) &= |S_2(P) - S_3(P)| \\ &= |S_1(P) - 2 \cdot S_3(P)|. \end{aligned} \tag{24}$$

where $S_3(P) = \int_0^1 L(P)dP$, $S_2(P) = S_1 - S_3(P)$ . $S_1$ is a fixed constant 1/2.

We have seen from the (24) that the larger the $\delta(P)$ value, the greater the difference between the area $S_2$ and $S_3$. In that case, we calculate 256 area differences as Fig. 5. (Note that in Fig. 2, the hue level has been quantized to 256 levels.)

Fig. 5 shows the different linearized histograms with three different breakpoints (5, 57) on circular histogram. From Fig. 5(a), the breakpoint $t_1 = 5$ is the maximum point of the area difference point, while $t_1 = 57$ is the minimum value of the area difference. We have seen that the Fig. 5(b) is the most similar to the original distribution. Thereby, we can break the circular histogram at the maximum value of the area difference.

#### 3) RELATION BETWEEN AREA DIFFERENCE AND DIRECTIONS

Also, the expansion in CW clockwise (CW) direction case and the relation between the area difference and the expansion direction should be discussed.

In order to analyze the relation between area difference and search direction, we have also calculated the area difference in clockwise (CW) CW direction as shown in Fig. 6.

As shown in Fig. 6, the area difference $\delta$ in CW direction varies with the change of the breakpoints, and the minimum value corresponds to 160, while the maximum value to 180. We have tested the histogram distribution state at the breakpoint $t_1 = 160$ as Fig. 6(b) shows. With the criteria that we propose, the Fig. 6(b) can be the optimal expansion result in CW direction.

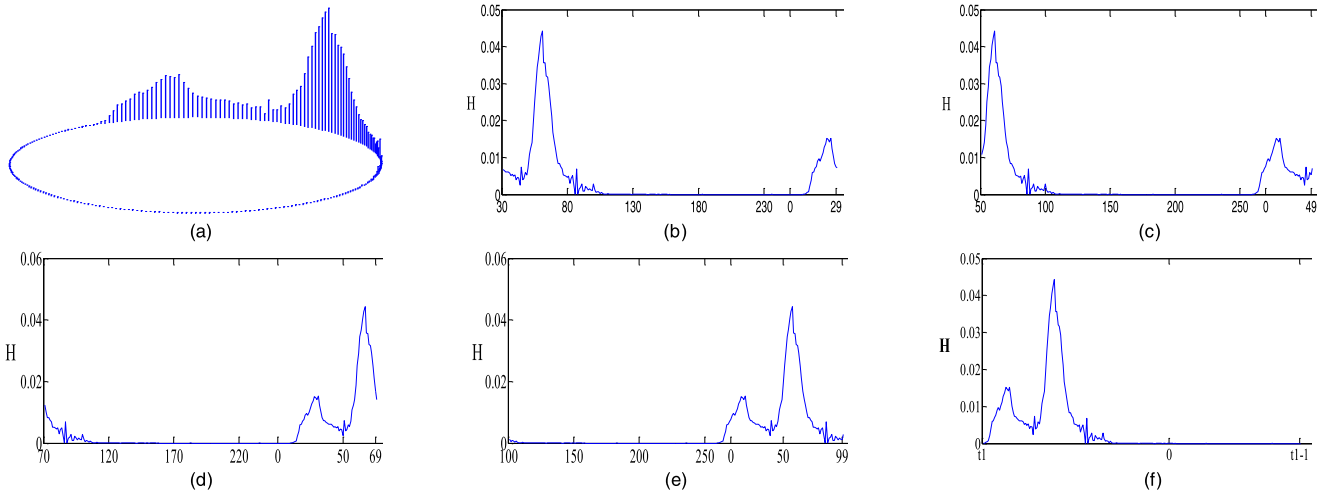


**FIGURE 3.** Circular histogram's expansion at four positions. (a) Circular histogram. (b) $t = 30$. (c) $t = 50$. (d) $t = 70$. (e) $t = 100$. (f) ideal histogram.

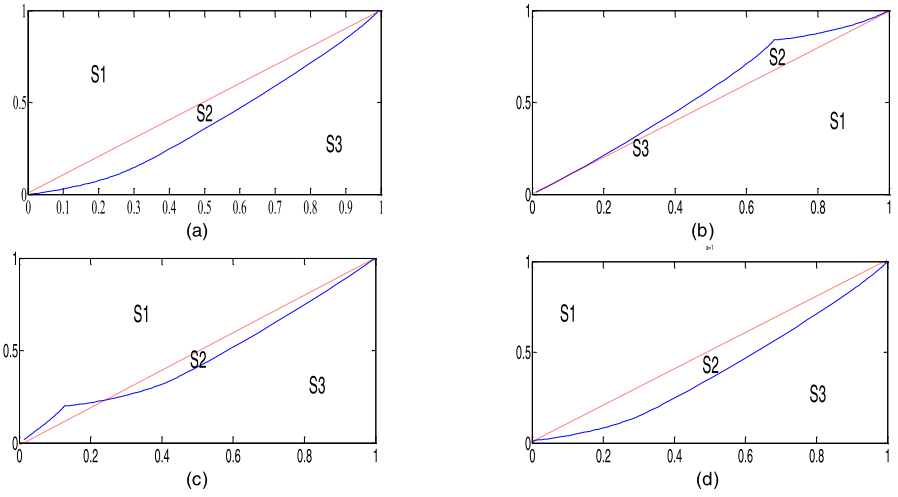


**FIGURE 4.** Lorenz curve at four points in ACW direction. (a) $t = 30$. (b) $t = 50$. (c) $t = 70$. (d) $t = 100$.

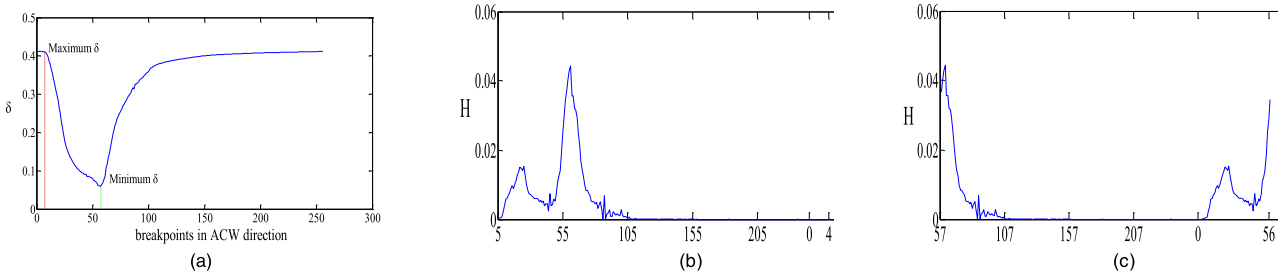


**FIGURE 5.** The linearized histogram based on area difference in ACW direction. (a) area difference (b) linearized histogram at maximum threshold 5 (c) linearized histogram at minimum point 57.

Therefore, the expansion breakpoints $t^*_{1ACW}$ and $t^*_{1CW}$ of the circular histogram in two directions are as follows:

$$t^*_{1ACW} = \arg \max_{0 \le P \le 1} \delta_{ACW}(P(t_{1ACW})), \tag{25}$$

or in the CW direction:

$$t^*_{1CW} = \arg \max_{0 \le P \le 1} \delta_{CW}(P(t_{1CW})). \tag{26}$$

### C. CIRCULAR HISTOGRAM LINEARIZING MODEL

In the expansion process, we found there are two different directions for expansion. In that case, the hue value $t = 0, 1, \ldots, 255$ (Note that we have quantized the hue levels to 256 levels) on circular histogram denotes searching in anti-clockwise (ACW) direction. The clockwise (CW) direction denotes the opposite situation.

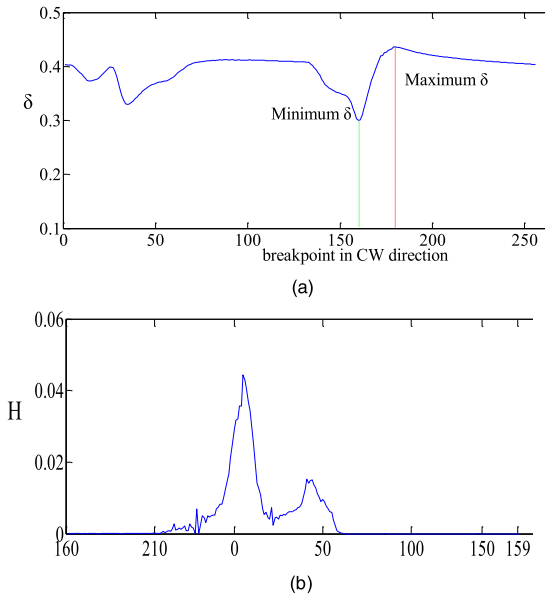


**FIGURE 6.** The linearized histogram based on area difference in CW direction. (a) area difference (b) linearized histogram at 160 point.

The linearized histogram

$$\{h(t_1), h(t_1+1), \ldots, h(255), h(0), \ldots, h(t_1-1)\}$$

satisfies $\sum_{t=t_1}^{\circ t_1-1} h(t) = 1(h(t) \geq 0)$.

Denoting the linearized histogram of two different directions as $h_{ACW}(t, t_1)$ and $h_{CW}(t, t_1)$. So:

$$h_{ACW}(t, t_1) = h((t + t_1) \bmod 256), \tag{27}$$
$$h_{CW}(t, t_1) = h((256 - (t - t_1)) \bmod 256), \tag{28}$$

where $t_1$ is the breakpoint on circular histogram, $t, t_1 \in \{0, 1, \ldots, L-1\}$.

Therefore, the new linearized histograms in two different directions are obtained as:

$$h_{ACW}(t, t^*_{1ACW}) = h((t + t^*_{1ACW}) \bmod 256), \tag{29}$$
$$h_{CW}(t, t^*_{1CW}) = h((256 - (t - t^*_{1CW})) \bmod 256), \tag{30}$$

## V. ENTROPY THRESHOLDDING ALGORITHM ON LINEARIZED CIRCULAR HISTOGRAM

In ACW direction case, based on this new linearized histogram (29), denoting the threshold as $t_2$, the cumulative probabilities of the two parts now is obtained as:

$$P_0(t^*_{1ACW}, t_2) = \sum_{t=0}^{\circ t_2} h_{ACW}(t, t^*_{1ACW}), \tag{31}$$
$$P_1(t^*_{1ACW}, t_2) = \sum_{t=t_2+1}^{\circ t^*_{1ACW}-1} h_{ACW}(t, t^*_{1ACW}). \tag{32}$$

The entropy of the entire image objective function $H_{TACW}(t^*_{1ACW}, t_2) = H_0(t^*_{1ACW}, t_2) + H_1(t^*_{1ACW}, t_2)$ is

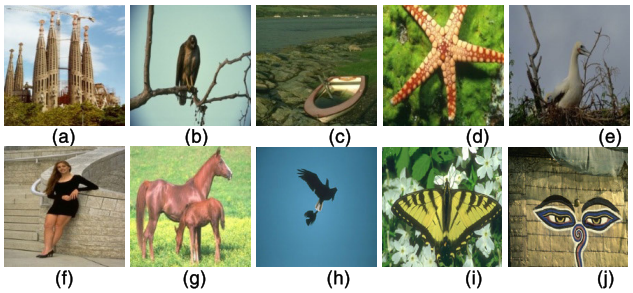


**FIGURE 7.** Color images in Berkeley database. (a) Tower. (b) Owl. (c) Boat. (d) Starfish. (e) Duck. (f) Women. (g) Horse. (h) Eagle. (i) Butterfly. (j) Mask.

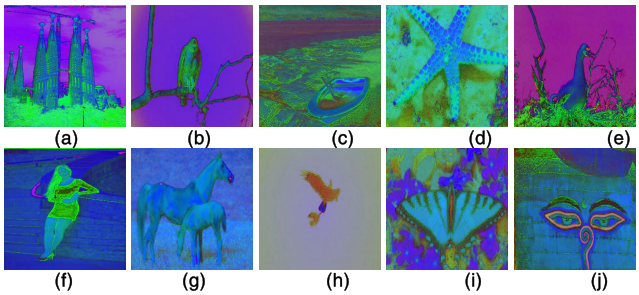


**FIGURE 8.** Color images in HSI color space. (a) Tower. (b) Owl. (c) Boat. (d) Starfish. (e) Duck. (f) Women. (g) Horse. (h) Eagle. (i) Butterfly. (j) Mask.

obtained:

$$\begin{aligned} H_{TACW}(t^*_{1ACW}, t_2) &- \sum_{t=0}^{\circ t_2} \frac{h_{ACW}(t, t^*_{1ACW})}{P_0(t^*_{1ACW}, t_2)} \log \frac{h_{ACW}(t, t^*_{1ACW})}{P_0(t^*_{1ACW}, t_2)} \\ &- \sum_{t=t_2+1}^{\circ t^*_{1ACW}-1} \frac{h_{ACW}(t, t^*_{1ACW})}{P_1(t^*_{1ACW}, t_2)} \log \frac{h_{ACW}(t, t^*_{1ACW})}{P_1(t^*_{1ACW}, t_2)}. \end{aligned} \tag{33}$$

Therefore, the optimal threshold $t^*_2$ is obtained as:

$$t^*_2(t^*_{1ACW}) = \arg\max_{t_2 \in \eta} H_{TACW}(t^*_{1ACW}, t_2). \tag{34}$$

where $\eta = \{t^*_{1ACW}, t^*_{1ACW}+1, \ldots, 255, 0, \ldots, t^*_{1ACW}-1\}$.

As for CW direction case, the optimal threshold $t^*_2$ is:

$$t^*_2(t^*_{1CW}) = \arg\max_{t_2 \in \gamma} H_{TCW}(t^*_{1CW}, t_2). \tag{35}$$

where $\gamma = \{t^*_{1CW}, t^*_{1CW}-1, \ldots, 0, 255, \ldots, t^*_{1ACW}+1\}$.

The process of entropy thresholding on linearized histogram in ACW direction is described as follows:

1) Transferring the images in RGB color space into HSI color space and obtaining the circular histogram $h(t)$ of H component.
2) Denoting the breakpoint $t_1 = 0, 1, \ldots, L-1$ on circular histogram and breaking the circular histogram at all the breakpoints into the linearized histogram $h_{ACW}(t, t_1)$ (27).
3) Once a starting point $t_1$ is selected, using the index of area difference $\delta(P)$ (24) in Lorenz curve to evaluate

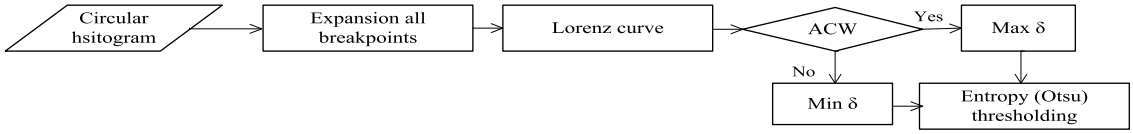


**FIGURE 9.** The flow chart of the experimental process.

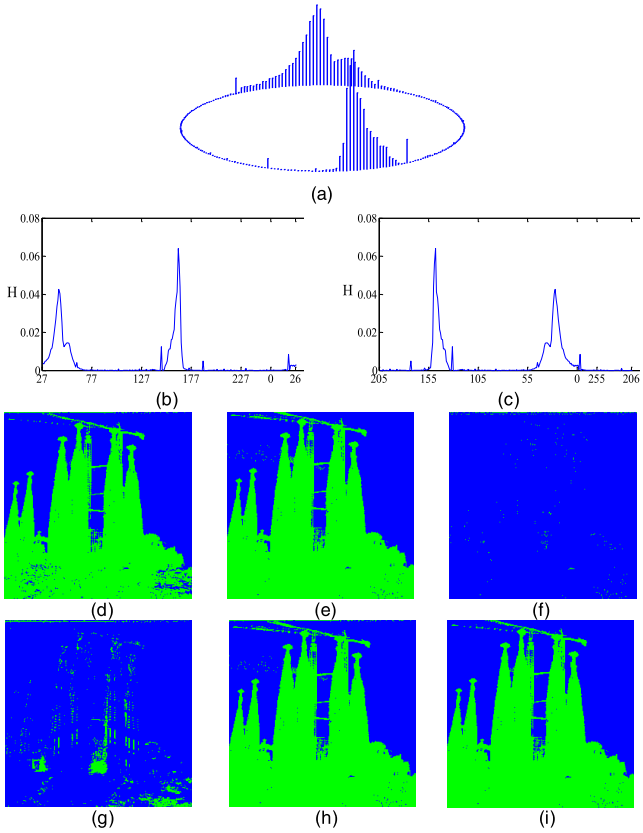


**FIGURE 10.** (a) circular histogram. (b) linearized histogram (ACW). (c) linearized histogram (CW). (d) Otsu circular thresholding (e) entropy circular thresholding. (f) Lorenz Otsu thresholding (CW). (g) Lorenz entropy thresholding (CW). (h) Lorenz Otsu thresholding (ACW). (i) Lorenz entropy thresholding (ACW).

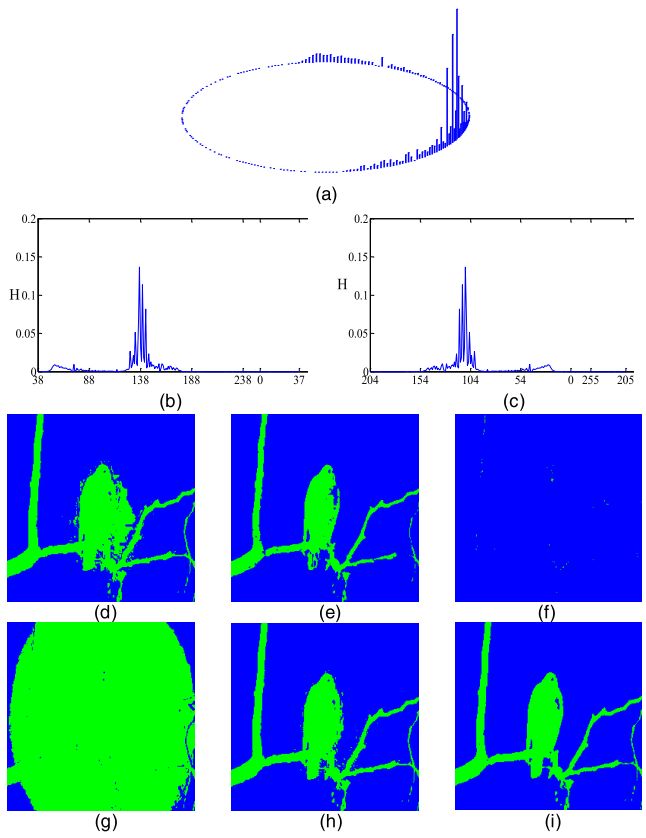


**FIGURE 11.** (a) circular histogram. (b) linearized histogram (ACW). (c) linearized histogram (CW). (d) Otsu circular thresholding (e) entropy circular thresholding. (f) Lorenz Otsu thresholding (CW). (g) Lorenz entropy thresholding (CW). (h) Lorenz Otsu thresholding (ACW). (i) Lorenz entropy thresholding (ACW).

all the 256 linearized histograms, and then choose the optimal histogram $h_{ACW}(t, t^*_{1ACW})$ (29), satisfying the maximum area difference index.

4) Using entropy thresholding method on the selected optimal histogram $h_{ACW}(t, t^*_{1ACW})$ to obtain the entropic threshold $t^*_2(t^*_{1ACW})$ (34), and finally segmenting the H component.

Similarly, the major process of entropy thresholding on linearized histogram in CW direction is almost the same as that of entropy thresholding on linearized histogram in ACW direction. However, the differences between two processes are in Step 2 and Step3. The linearized histogram $h_{CW}(t, t_1)$ (28) would be the opposite of that in ACW direction case in Step 2, and the breakpoint $t_1$ searches the CW direction. Also, the optimal index of area difference $\delta(P)$ in Lorenz curve selects the minimum value to obtain the optimal histogram $h_{CW}(t, t^*_{1CW})$ (30). Finally, we obtain the optimal entropic threshold $t^*_2(t^*_{1CW})$ (35) in CW direction case.

## VI. EXPERIMENT RESULTS AND ANALYSIS

In order to evaluate the performance of our proposed methods, all the experiments are simulated on PC with Matlab (2014 version) on H component.

The experiments have been designed to contain circular histogram thresholding models of two types: Otsu-based circular thresholding by within-class variance (11), entropy-based circular thresholding (19), Lorenz curve-based entropy linear thresholding in ACW direction (34), and that in CW

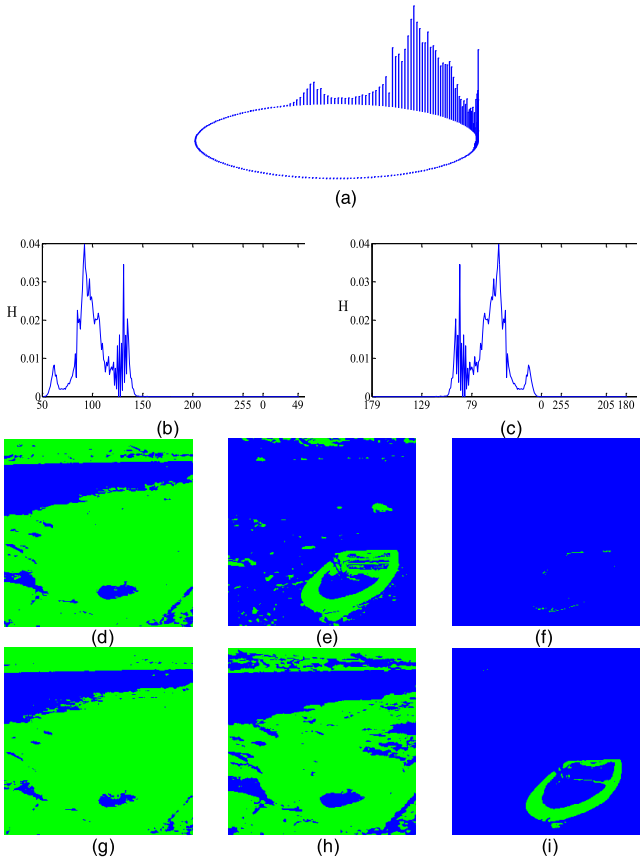


**FIGURE 12.** (a) circular histogram. (b) linearized histogram (ACW). (c) linearized histogram (CW). (d) Otsu circular thresholding (e) entropy circular thresholding. (f) Lorenz Otsu thresholding (CW). (g) Lorenz entropy thresholding (CW). (h) Lorenz Otsu thresholding (ACW). (i) Lorenz entropy thresholding (ACW).

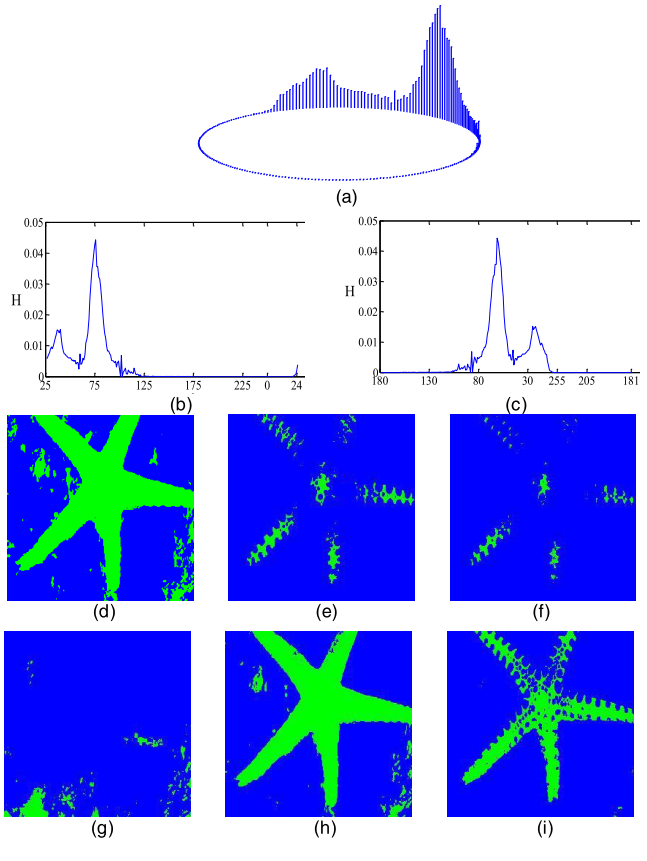


**FIGURE 13.** (a) circular histogram. (b) linearized histogram (ACW). (c) linearized histogram (CW). (d) Otsu circular thresholding (e) entropy circular thresholding. (f) Lorenz Otsu thresholding (CW). (g) Lorenz entropy thresholding (CW). (h) Lorenz Otsu thresholding (ACW). (i) Lorenz entropy thresholding (ACW).

direction (35). It is shown that the Lorenz curve-based entropy linear thresholding can obtain better segmentation result. As compared, we also test the Lorenz curve-based linear thresholding with Otsu method.

The experimental data is contained in Fig. 7 and Fig. 8. Fig. 7(a)-(j) is the color images in RGB color space from the Berkeley database. Fig. 8(a)-(j) are the exhibitions in HSI color space, which have different periodic distributions. For the convenience, the following experiments Otsu-based circular thresholding by within-class variance, entropy-based circular thresholding, Lorenz curve-based Otsu linear thresholding, Lorenz curve-based entropy linear thresholding and are simply noted as Otsu circular thresholding, entropy circular thresholding, Lorenz Otsu thresholding (ACW or CW) and Lorenz entropy thresholding (ACW or CW).

The whole experimental process is shown as Fig. 9:

As we can see from Fig. 10 (a), the circular histogram shows the bimodal distribution with a little difference between the two classes. The optimal breakpoint is supposed to lie at the left side of the small peak, so the threshold would be selected in the middle of the two peaks. In this case, the Otsu method can be applied to this histogram type with little difference of the segmentation result to that of the entropy thresholding.

Comparing with the results of Fig. 10(d)-(i), the entropy-based results from Fig. 10(e) and Fig. 10(i) show the better effect.

From Fig. 11 (a), we can see that the hues' distribution is close to unimodal where the Otsu method is not suitable for thresholding on this histogram type. The entropy-based method shows better adaptability. The optimal breakpoint is not supposed to destroy the original distribution of the circular histogram.

From Fig. 11(d), (f) and (h), we can know that the results of Otsu-based method cannot segment the hues appropriately.

We have seen from Fig. 12 (a), the circular histogram is close to the bimodal, however, the distribution of the two classes shows a lot of difference. This distribution may not be appropriate for using the Otsu method.

Fig. 12 (d) and (e) have shown that the segmentation result of entropy circular thresholding is better that of the Otsu circular thresholding. That shows the good properties of the entropy method. From Fig. 12(i), the Lorenz entropy thresholding (ACW) had obtained the best segmentation result.

As shown in Fig. 13 (a), the circular histogram has two clear peaks with the difference. Fig. 13(d), (f) and (h) all show

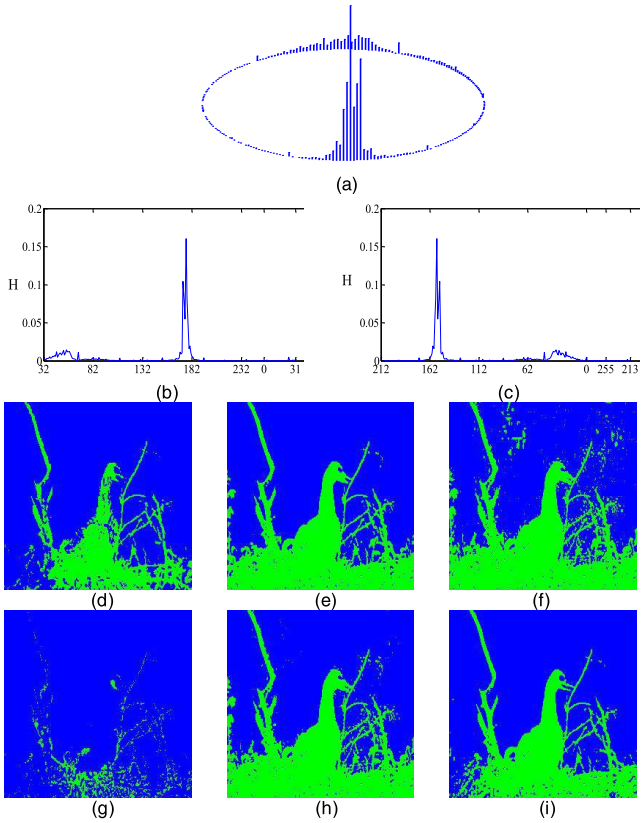


**FIGURE 14.** (a) circular histogram. (b) linearized histogram (ACW). (c) linearized histogram (CW). (d) Otsu circular thresholding (e) entropy circular thresholding. (f) Lorenz Otsu thresholding (CW). (g) Lorenz entropy thresholding (CW). (h) Lorenz Otsu thresholding (ACW). (i) Lorenz entropy thresholding (ACW).

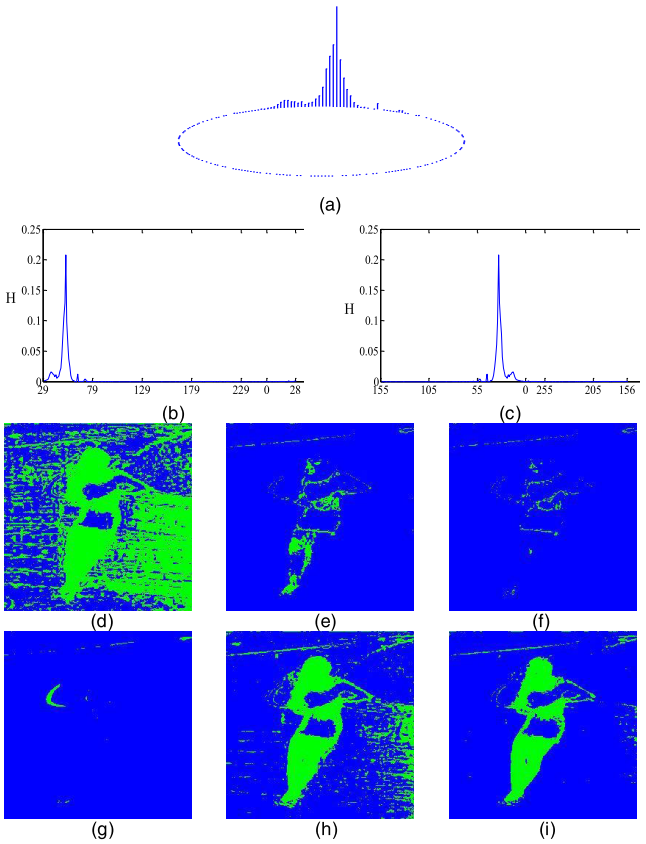


**FIGURE 15.** (a) circular histogram. (b) linearized histogram (ACW). (c) linearized histogram (CW). (d) Otsu circular thresholding (e) entropy circular thresholding. (f) Lorenz Otsu thresholding (CW). (g) Lorenz entropy thresholding (CW). (h) Lorenz Otsu thresholding (ACW). (i) Lorenz entropy thresholding (ACW).

that the Otsu method is not suitable for thresholding on the distribution with large difference, and demonstrates that the proposed method can maintain the original distribution. The threshold selected by the Otsu method may bias the larger one.

We can observe intuitively from Fig. 14(a) that the histogram is bimodal that the two classes have large differences. In this case, from Fig. 14(d) and (e), entropy thresholding can obtain the better segmentation effect than that of the Otsu method.

From Fig. 14(i) we can know that Lorenz entropy thresholding (ACW) segmented the target most clearly. The Otsu-based method from Fig. 14(d), (f) and (h) show low effectiveness.

The histogram in Fig. 15(a) is shown as unimodal, and the threshold selected by Otsu method may be in the middle section of the peak. From Fig. 15(d) and (e), the segmentation result by the Otsu-based method cannot isolate the target. Fig. 15(i) demonstrates that the result by Lorenz entropy thresholding can obtain a better result than that of entropy circular thresholding.

From Fig. 16(a), we can see that this circular histogram of Fig. 8(g) is nearly bimodal distribution. The optimal threshold is supposed to be at the valley between the two peaks, and the breakpoint should be at any point except the peaks. Therefore, the Otsu method may be well used in it from Fig. 16(d), with little difference between Fig. 16(e). We can see from Fig. 16(h) and (i), the Otsu-based method can obtain a better result in this bimodal case.

Fig. 17 (a) shows the unimodal case of the histogram, and we can see from Fig. 17(d) that the Otsu method cannot segment the target correctly. Fig. 17 (f) had corrected the effect of the Otsu method to some extent. Fig. 17(g) had demonstrated the better adaptability of the entropy method.

We can see from Fig. 18(i), the number of the pixels of the two classes is not similar, and two classes of the histogram show unequal variance. In that case, the Otsu method may not segment the target appropriately. From Fig. 18(e), we can see that the entropy thresholding can be applied on this case. Fig. 18(i) shows the best segmentation result.

Fig. 19 (a) shows that the unimodal histogram of hue values. In the comparison of Fig. 19 (d) and Fig. 19 (e), the entropy-based method can modify the segmentation result of that in Otsu thresholding. Fig. 19 (i) shows the best result of the Lorenz entropy thresholding method (ACW).

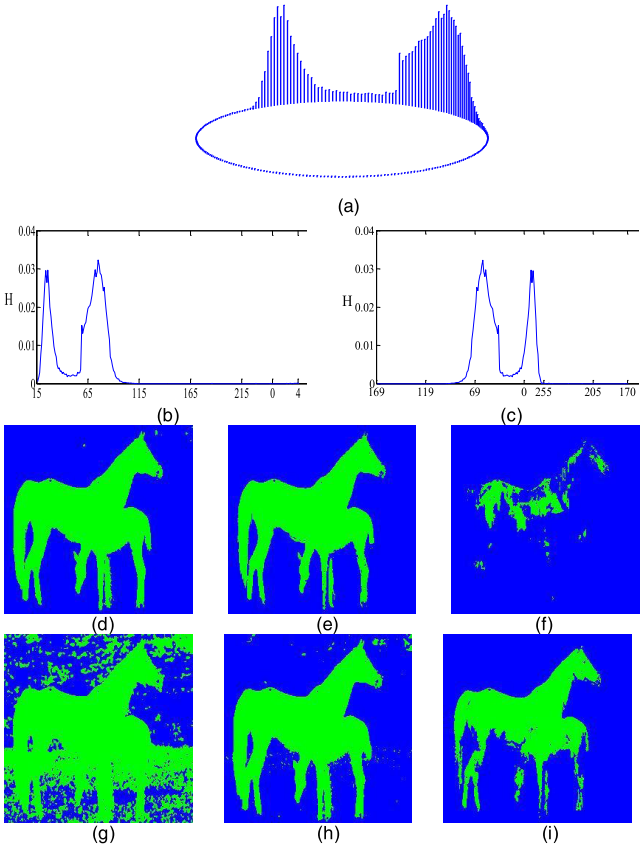


**FIGURE 16.** (a) circular histogram. (b) linearized histogram (ACW). (c) linearized histogram (CW). (d) Otsu circular thresholding (e) entropy circular thresholding. (f) Lorenz Otsu thresholding (CW). (g) Lorenz entropy thresholding (CW). (h) Lorenz Otsu thresholding (ACW). (i) Lorenz entropy thresholding (ACW).

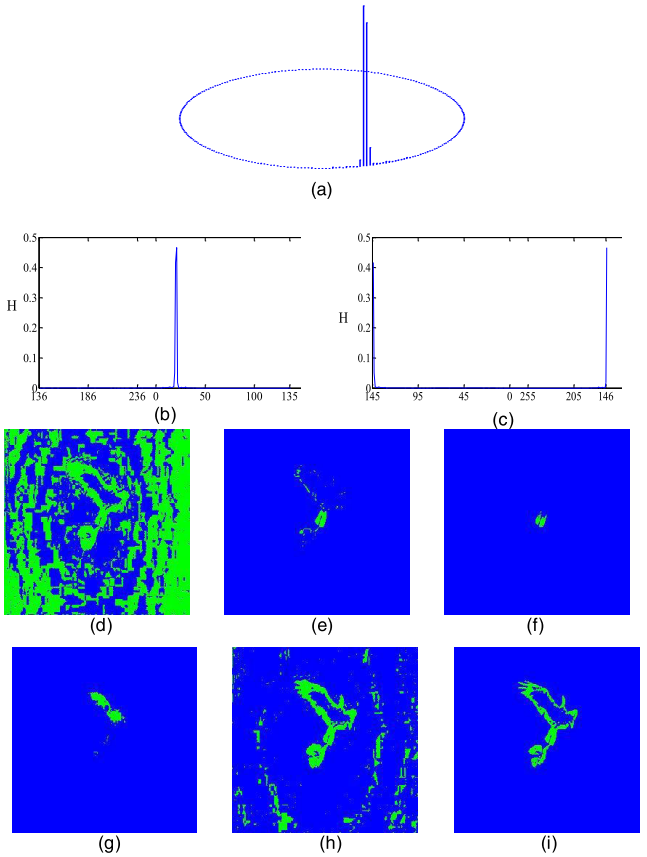


**FIGURE 17.** (a) circular histogram. (b) linearized histogram (ACW). (c) linearized histogram (CW). (d) Otsu circular thresholding (e) entropy circular thresholding. (f) Lorenz Otsu thresholding (CW). (g) Lorenz entropy thresholding (CW). (h) Lorenz Otsu thresholding (ACW). (i) Lorenz entropy thresholding (ACW).

All the segmentation results from Fig. 10-Fig.19 demonstrates that the entropy method can be well applied to the various distributions of the circular histogram. Lorenz entropy thresholding can be more adaptable. Also, images (f) and (g) from Fig.10-Fig. 19 had shown the low effect of the Lorenz curve-based thresholding method in CW direction.

In order to evaluate the effectiveness of the proposed method, considering the poor results of the methods in CW direction, we only use the evaluation indexes [24] of image segmentation to evaluate the segmentation results in ACW direction.

Table 1 respectively shows the average value of speed, pixel accuracy (PA) value [25] and structural similarity (SSIM) value [26] of all the segmentation results of four thresholding methods in ACW direction.

We can see from Table 1, Lorenz entropy thresholding had the highest PA and SSIM value. Based on these two indexes, Otsu circular thresholding may have the problems in segmenting hues value. However, the entropy method can modify the segmentation effect of the Otsu-based method on hues.

Fig. 20 depicts the Precision-recall curve [27] for the segmented images of the 10 images. The graph vividly describes the high effectiveness of the proposed method than that of other methods.

**TABLE 1.** Evaluation tests for various segmentation methods (ACW direction).

| Methods | Speed (:second) | PA (:%) | SSIM (:%) |
|---|---|---|---|
| Otsu circular thresholding | 1.1685 | 0.4546 | 0.4862 |
| Entropy circular thresholding | 13.6782 | 0.7105 | 0.6891 |
| Lorenz Otsu thresholding | 3.9304 | 0.6015 | 0.6170 |
| Lorenz entropy thresholding | 7.4458 | 0.9094 | 0.8926 |

Fig. 21 describes the average value of segmentation speed for the segmented images of the 10 images. We can see that the Otsu-based method shows higher segmentation efficiency taking less time from method 1 and method 3. However, compared with the Otsu-based methods, the entropy-based methods take a longer time. From Fig. 21 shows the method 4 takes less time than that of method 2, that is, the proposed

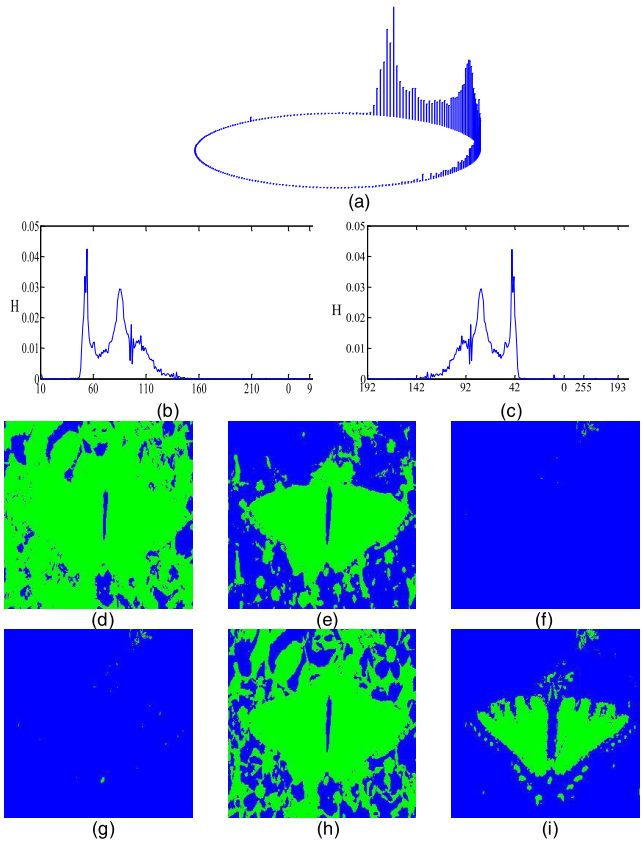


**FIGURE 18.** (a) circular histogram. (b) linearized histogram (ACW). (c) linearized histogram (CW). (d) Otsu circular thresholding (e) entropy circular thresholding. (f) Lorenz Otsu thresholding (CW). (g) Lorenz entropy thresholding (CW). (h) Lorenz Otsu thresholding (ACW). (i) Lorenz entropy thresholding (ACW).

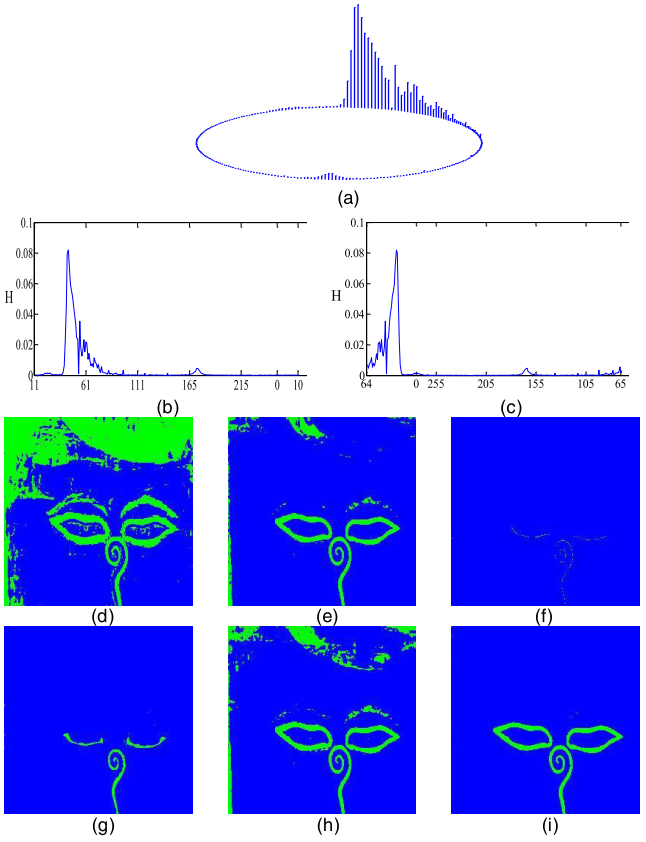


**FIGURE 19.** (a) circular histogram. (b) linearized histogram (ACW). (c) linearized histogram (CW). (d) Otsu circular thresholding (e) entropy circular thresholding. (f) Lorenz Otsu thresholding (ACW). (g) Lorenz entropy thresholding (ACW). (h) Lorenz Otsu thresholding (CW). (i) Lorenz entropy thresholding (CW).

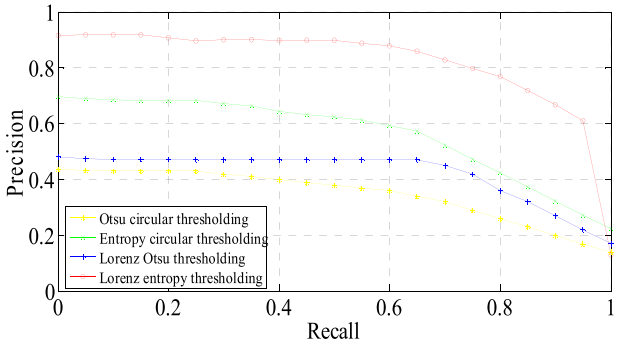


**FIGURE 20.** Precision-recall curves of segmented images obtained by different segmentation methods.

method has indeed reduced the complexity of entropy circular thresholding.

Fig. 22 shows that the segmentation results by two normal gray-level thresholding methods (Otsu and max entropy) on saturation and intensity value in HSI color space. However, Fig. 22(e)-Fig. 22(h) indicates that the poor segmentation performance on these two components whether by two different thresholding methods. Fig. 22(j) appears to have the better result in entropy thresholding on saturation component. From the above experiment, we can see that the two other components in HSI color space may not be considered as the single component for segmenting the color image. The thresholding methods can be used on both these three components separately, however, the three components converted from RGB color space may not be all considered as the representative of image information and the transformation process may have the significant change, which cause the unbalance among H, S and I components. Saturation is the measurement of how the hues are diluted in white light; Intensity is the brightness of the color information. In that case, using saturation and intensity component to be as the segmentation index may lead to the inappropriate results. Fig. 22(i)-Fig. 22(l) demonstrate the better results than that of Fig. 22(e)-Fig. 22(h).

Besides, these three components (hue, saturation and intensity) cannot be merged either due to the high irrelevant relation. In that case, this paper only utilizes the hue component, which describes a pure color, and this component can represent the whole color information and can be well used in achieving color information.

This paper has introduced a novel model of circular thresholding. In order to reduce the complexity of binary thresholding on circular histogram, unlike the efficient circular

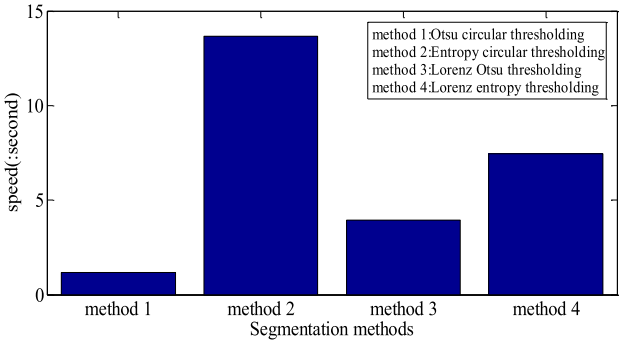


**FIGURE 21.** Speed of segmented images obtained by different segmentation methods.

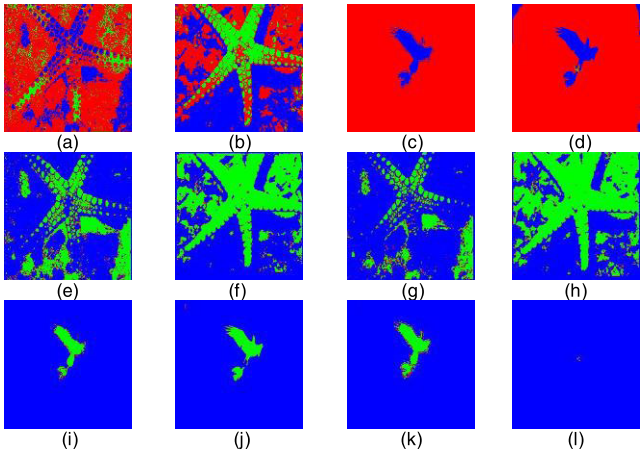


**FIGURE 22.** Segmentation results. (a) Saturation. (b) Intensity. (c) Saturation. (d) Intensity. (e) Saturation Otsu thresholding. (f) Saturation entropy thresholding. (g) Intensity Otsu thresholding. (h) Intensity entropy thresholding. (i) Saturation Otsu thresholding. (j) Saturation entropy thresholding. (k) Intensity Otsu thresholding. (l) Intensity entropy thresholding.

thresholding in literature [11], the optimal breakpoint on circular histogram is selected before the circular calculation to expand the circular histogram into the linearized histogram most similar to the original distribution. In that case, the Lorenz curve technique is utilized to measure the uniformity of all the linearized histograms (expanded from the circular histogram in two different directions), and then obtain the corresponding optimal breakpoint when only the linearized histogram satisfies the optimal index of Lorenz curve. All the experimental data demonstrate that the proposed method can achieve the better result, and actually reduced the complexity of binary thresholding in entropy-based circular thresholding. However, this proposed method has not been extended to the multi-threshold case, in that case, in future work we will modify the proposed method to extend to the multi-threshold case. Also, in order to reduce the complexity in the multi-threshold case to meet the real-time requirement, one of the automatic threshold selection methods, literature [28] shows a fast automatic optimal threshold selection technique with major practical application, and this technique may be referred into the proposed method in the paper in future work.

## VII. CONCLUSION

This paper presents a new method to solve the problem of the existing circular histogram thresholding, from which the proposed method gives a solution of thresholding on circular histogram of hues. Based on Lorenz curve technique and the unique periodic distribution of H component, the circular histogram is expanded with the optimal breakpoint as the starting point and we can obtain the optimal segmentation threshold by entropy method. The experimental results of the Lorenz entropy thresholding method proposed in this paper are better than other methods.

## REFERENCES

[1] H. Cheng, X. Jiang, Y. Sun, and J. Wang, "Color image segmentation: Advances and prospects," *Pattern Recognit.*, vol. 34, no. 12, pp. 2259–2281, Dec. 2001, doi: 10.1016/s0031-3203(00)00149-7.

[2] F. Garcia-Lamont, J. Cervantes, A. López, and L. Rodriguez, "Segmentation of images by color features: A survey," *Neurocomputing*, vol. 292, pp. 1–27, May 2018, doi: 10.1016/j.neucom.2018.01.091.

[3] R. Gothwal, S. Gupta, D. Gupta, and A. K. Dahiya, "Color image segmentation algorithm based on RGB channels," in *Proc. 3rd Int. Conf. Rel., Infocom Technol. Optim.*, Noida, India, Oct. 2014, pp. 1–5.

[4] S. Ito, M. Yoshioka, S. Omatu, K. Kita, and K. Kugo, "An image segmentation method using histograms and the human characteristics of HSI color space for a scene image," *Artif. Life Robot.*, vol. 10, no. 1, pp. 6–10, Jul. 2006, doi: 10.1007/s10015-005-0352-x.

[5] C. Zhang and P. Wang, "A new method of color image segmentation based on intensity and hue clustering," presented at the 15th Int. Conf. Pattern Recognit. Barcelona, Spain, Sep. 2000.

[6] Z. Y. Li, Z. C. Yu, W. X. Liu, and Z. C. Zhang, "Tongue image segmentation via color decomposition and thresholding," presented at the 4th Int. Conf. Inf. Sci. Control Eng., Changsha, China, Jul. 2017.

[7] T. Markchom and R. Lipikorn, "Thin cloud removal using local minimization and logarithm image transformation in HSI color space," presented at the 4th Int. Conf. Front. Signal Process., Sep. 2018.

[8] D.-C. Tseng, Y.-F. Li, and C.-T. Tung, "Circular histogram thresholding for color image segmentation," in *Proc. 3rd Int. Conf. Document Anal. Recognit.*, Montreal, QC, Canada, Nov. 2002, pp. 637–676.

[9] J. Wu, P. Zeng, Y. Zhou, and C. Olivier, "A novel color image segmentation method and its application to white blood cell image analysis," in *Proc. 8th Int. Conf. Signal Process.*, Beijing, China, Nov. 2006, p. 2.

[10] D. Dimov and L. Laskov, "Cyclic histogram thresholding and multithresholding," in *Proc. Int. Conf. Comput. Syst. Technol. Workshop PhD Students Comput.*, Rousse, Bulgaria, Jun. 2009, Art. no. 18.

[11] Y.-K. Lai and P. L. Rosin, "Efficient circular thresholding," *IEEE Trans. Image Process.*, vol. 23, no. 3, pp. 992–1001, Mar. 2014, doi: 10.1109/TIP.2013.2297014.

[12] N. Otsu, "A threshold selection method from gray-level histograms," *IEEE Trans. Syst., Man, Cybern.*, vol. SMC-9, no. 1, pp. 62–66, Jan. 1979, doi: 10.1109/tsmc.1979.4310076.

[13] K. Fujita, "A clustering method for data in cylindrical coordinates," *Math. Problems Eng.*, vol. 2017, pp. 1–11, Sep. 2017, doi: 10.1155/2017/3696850.

[14] T. Kurita, N. Otsu, and N. Abdelmalek, "Maximum likelihood thresholding based on population mixture models," *Pattern Recognit.*, vol. 25, no. 10, pp. 1231–1240, Oct. 1992, doi: 10.1016/0031-3203(92)90024-d.

[15] X. Xu, S. Xu, L. Jin, and E. Song, "Characteristic analysis of Otsu threshold and its applications," *Pattern Recognit. Lett.*, vol. 32, no. 7, pp. 956–961, May 2011, doi: 10.1016/j.patrec.2011.01.021.

[16] J. Kittler and J. Illingworth, "On threshold selection using clustering criteria," *IEEE Trans. Syst., Man, Cybern.*, vols. SMC–15, no. 5, pp. 652–655, Sep. 1985, doi: 10.1109/tsmc.1985.6313443.

[17] J. Kapur, P. Sahoo, A. Wong, "A new method for gray-level picture thresholding using the entropy of the histogram," *Signal. Process.*, vol. 2, no. 3, pp. 273–285, Jul. 1980.

[18] J. L. Gastwirth, "A general definition of the lorenz curve," *Econometrica*, vol. 39, no. 6, p. 1037, Nov. 1971, doi: 10.2307/1909675.
[19] P. Shih and C. Liu, "Comparative assessment of content-based face image retrieval in different color spaces," *Int. J. Patt. Recogn. Artif. Intell.*, vol. 19, no. 7, pp. 873–893, Nov. 2005, doi: 10.1142/s0218001405004381.
[20] M. Cote and A. B. Albu, "A comparative study of sparseness measures for segmenting textures," in *Proc. 13th Conf. Comput. Robot Vis. (CRV)*, Victoria, BC, Canada, Jun. 2016, pp. 186–193.
[21] M. Habba, M. Ameur, and Y. Jabrane, "A novel Gini index based evaluation criterion for image segmentation," *Optik*, vol. 168, pp. 446–457, Sep. 2018, doi: 10.1016/j.ijleo.2018.04.045.
[22] A. C. Silva, P. C. P. Carvalho, and M. Gattass, "Diagnosis of lung nodule using Gini coefficient and skeletonization in computerized tomography images," in *Proc. ACM Symp. Appl. Comput.*, Nicosia, Cyprus, Mar. 2004, pp. 243–248.
[23] S. Goswami, C. Murthy, and A. K. Das, "Sparsity measure of a network graph: Gini index," *Inf. Sci.*, vol. 462, pp. 16–39, Sep. 2018, doi: 10.1016/j.ins.2018.05.044.
[24] Y. Zhang, "A survey on evaluation methods for image segmentation," *Pattern Recognit.*, vol. 29, no. 8, pp. 1335–1346, Aug. 1996, doi: 10.1016/0031-3203(95)00169-7.
[25] G. M. Foody, "Status of land cover classification accuracy assessment," *Remote Sens. Environ.*, vol. 80, no. 1, pp. 185–201, Apr. 2002, doi: 10.1016/s0034-4257(01)00295-4.
[26] Z. Wang, A. C. Bovik, H. R. Sheikh, and E. P. Simoncelli, "Image quality assessment: From error visibility to structural similarity," *IEEE Trans. Image Process.*, vol. 13, no. 4, pp. 600–612, May 2004, doi: 10.1109/TIP.2003.819861.
[27] X. Zhang, X. Feng, P. Xiao, G. He, and L. Zhu, "Segmentation quality evaluation using region-based precision and recall measures for remote sensing images," *ISPRS J. Photogram. Remote Sens.*, vol. 102, pp. 73–84, Apr. 2015, doi: 10.1016/j.isprsjprs.2015.01.009.
[28] A. Singla and S. Patra, "A fast automatic optimal threshold selection technique for image segmentation," *SIViP*, vol. 11, no. 2, pp. 243–250, Feb. 2017, doi: 10.1007/s11760-016-0927-0.

**CHAO KANG** was born in Baoji, Shaanxi, in November 1992. He is currently pursuing the M.S. degree with the School of Communication and Information Engineering, Xi'an University of Posts and Telecommunications. His research interest includes color image analysis and image processing.

**CHENGMAO WU** was born in Yilong, Sichuan, in October 1968. He received the bachelor's degree in computer applications.

From 1992 to 1995, he was engaged in the research of launch vehicle and intercontinental missile test technology at the 11th Institute of the Sixth Research Institute of the Ministry of Space. Since 1996, he has been engaged in teaching and scientific research with the School of Electronic Information Engineering and the School of Electronic Engineering, Xi'an University of Posts and Telecommunications. He is currently a Senior Engineer and a Master's Tutor in circuit and systems, and electronic and communication engineering with the School of Electronic and Communication Engineering, Xi'an University of Posts and Telecommunications. He has hosted and participated in the 11 kinds of national projects, also published more than 200 academic articles in China and abroad. His research interests include the pattern analysis and intelligent information processing, image processing and information security, non-linear dynamic systems, chaotic electronics, chaotic secure communication, modern non-linear circuit analysis theory, fractional impedance circuit, intelligent management, and decision-making. He is a member of China Democratic League.

**JIULUN FAN** was born in November 1964. He received the Ph.D. degree in signal and information processing from the School of Electronic Engineering, Xi'an University of Electronic Science and Technology, in March 1998.

From 1998 to 2000, he worked in the Postdoctoral Mobile Station, Northwest Polytechnic University. He is currently the President of the Xi'an University of Posts and Telecommunications. He is a Second-Level Professor. In recent years, the main achievements are as follows: More than ten national and provincial scientific research projects, such as the National Natural Science Foundation, the National 242 Information Security Plan and so on, have published more than 150 academic articles in domestic and foreign journals and conferences. He has published the academic monograph *Fuzzy Entropy Theory* and textbook *Basis of Cryptography*. His research interest includes fuzzy mathematics theory and fuzzy systems, uncertainty reasoning, pattern recognition and image processing, intelligent information processing, information security, fuzzy set theory, pattern recognition, and signal and information processing.

Dr. Fan has won the first prize in science and technology from the China Communication Society, the first prize in electronic information science and technology from the China Electronics Society, the second prize in science and technology in Shaanxi, the second prize in science and technology from Shaanxi University, and the third prize in science and technology six times.